Journal of Materials Chemistry

Cite this: *J. Mater. Chem.*, 2011, **21**, 8052

www.rsc.org/materials

PAPER

Silica-based complex nanorattles as multifunctional carrier for anticancer drug†

Yong Hu,*[a] Xin Ting Zheng,[b] Jun Song Chen,[b] Mojiao Zhou,[a] Chang Ming Li[b] and Xiong Wen (David) Lou*[b]

Received 11th March 2011, Accepted 8th April 2011
DOI: 10.1039/c1jm11060h

In this work, we demonstrate a new route to generate silica-based multifunctional complex nanorattles. By using SnO_2 hollow nanospheres as the starting template, we are able to build a new type of rattle-in-ball hollow structure with multi-level interior architecture, where the core of a nanorattle is itself another smaller rattle. Moreover, additional functionality can be introduced by forming Au nanoparticles in the interstitial space. Such unique hollow nanostructures are believed to be very useful as nanoreactors for selective catalysis. Magnetic functionality can also be incorporated by using an α-Fe_2O_3 nanospindle as the starting template followed by *in situ* reduction to Fe_3O_4. This type of ellipsoidal nanorattle is feasible for drug delivery as it is shown to be highly biocompatible and non-cytotoxic. The cell viability assay proves that the sample is an efficient drug delivery vehicle exhibiting similar anticancer efficacy against MCF-7 carcinoma cells as compared to the free DOX. By constructing these two types of complex nanorattles as examples, we demonstrate new possible routes to generate versatile hollow nanostructures with distinct architectures and chemical compositions, thus widening their application potential.

1. Introduction

Hollow nanostructures are of increasing importance in many applications. The most straightforward synthetic approach is the synthesis of core-shell nanoparticles with subsequent selective removal of the inner core.[1] One facile way of coating the core materials is by a layer-by-layer (LbL) adsorption technique, where multilayered polyelectrolyte is deposited on colloidal particles through electrostatic interaction.[2] Using this method, a wide range of hollow nanomaterials have been generated with a variety of physicochemical properties.[3–5] A significant development in hollow structures is the successful synthesis of more challenging rattle-type hollow particles. In a general synthesis, a functional core is first coated with an intermediate layer followed by an outer shell. Afterwards, the intermediate layer is selectively removed, leaving behind a movable core inside the shell.[6–8] Compared to the traditional hollow nanomaterials, this type of unique nanostructure can provide additional functionality by encapsulating a movable core inside the shell. Because of the functionalization of the interior,[9] this type of "nanorattle" quickly received enormous attention for its possible application in many fields such as nanoreactors and catalysis.[6,7,10–12]

Even though template-free methods are available to generate hollow or rattle-type structures,[13–16] the "bottom-up" approach is still widely practised,[17–20] as it provides the advantages of producing narrow-size-distribution colloids, and control over the shape of the final product.[21–26] Previously we created rattle-type silica (SiO_2) hollow nanospheres with multiple gold cores using polystyrene as templates.[10] Despite the fact that nanorattles with the core and shell contributing distinct functionalities have been fabricated,[27] the strategy by which such structures are achieved is generally the same as the original bottom-up approach. This presents a possible limitation that has to be overcome in order to further unveil the potential of these intriguing hollow nanostructures. Thus, new concepts for the fabrication of complex hollow structures are worth exploring further. Recently, Tang's group demonstrated an interesting approach to generate uniform nanorattles with both the core and shell made of SiO_2,[28] they also showed that Au nanoparticles with tunable sizes can be incorporated into the interstitial space of the rattle structure.[29] This presents an opportunity to fabricate complex nanorattles with multifunctional cores.

In this work, we demonstrate a new method to synthesize two types of silica-based nanorattles with multiple functionalities. As illustrated in Fig. 1, using tin dioxide (SnO_2) hollow nanospheres as the starting template, we are able to generate a new rattle-in-ball complex hollow structure, where the core of the larger rattle ($Sn@SiO_2@SiO_2$) is itself a smaller rattle ($Sn@SiO_2$). Moreover,

[a]*Zhejiang Key Laboratory for Reactive Chemistry on Solid Surfaces and Institute of Physical Chemistry, Zhejiang Normal University, Jinhua, 321004, P. R. China. E-mail: yonghu@zjnu.edu.cn*
[b]*School of Chemical and Biomedical Engineering, Nanyang Technological University, 70 Nanyang Drive, Singapore, 637457, Singapore. E-mail: xwlou@ntu.edu.sg*

† Electronic supplementary information (ESI) available: X-ray diffraction patterns, energy-dispersive X-ray analysis, N_2 adsorption–desorption isotherms and pore size distribution of the samples. See DOI: 10.1039/c1jm11060h

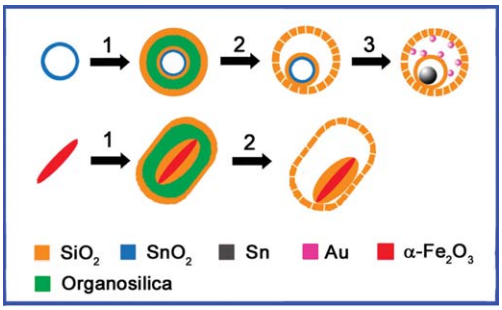

Fig. 1 Schematic illustration of the fabrication of complex rattle-type structures. Step 1: coating the template with SiO_2-organosilica-SiO_2 tri-layer. Step 2: selective removal of organosilica with HF. Step 3: introducing Au nanoparticles in the interstitial space of the rattle-type structure and subsequent reduction of SnO_2 to Sn.

the interstitial space between the inner and outer SiO_2 shells can be facilely functionalized with Au nanoparticles. This would probably be the first demonstration of a complex rattle structure with core materials composed of distinct chemical species (metallic Sn and multiple Au nanoparticles) which are individually confined in the sub-compartment of the hollow cavity, separated by the inner SiO_2 shell. The analogous structure of non-spherical α-Fe_2O_3@SiO_2@SiO_2 can also be formed by using α-Fe_2O_3 nanospindle as the starting template. After an *in situ* reduction of the α-Fe_2O_3 inner core to magnetite, Fe_3O_4@SiO_2@SiO_2 structures with a mesoporous outer SiO_2 shell[28] are obtained, which can be used as a multifunctional carrier for anticancer drugs.

2. Experimental

Synthesis of nano-templates

SnO_2@SnO_2 double-shell hollow nanospheres were synthesized following our previous method.[22] Briefly, SiO_2 nanospheres with ~200 nm diameter were first synthesized by the Stöber method.[22] Then, 0.25 g of these SiO_2 spheres were dispersed in 50 ml of a mixed solvent containing ethanol and H_2O at a volume ratio of 3 : 5, followed by the addition of 1.5 g of urea, and then 0.2 g of potassium stannate trihydrate. The reaction medium was then hydrothermally treated at 170 °C for 36 h. The process was repeated by using the as-prepared SiO_2@SnO_2 as the template. The obtained SiO_2@SnO_2@SnO_2 sample was then calcined at 600 °C in air for 2 h, after which the SiO_2 core was removed by dissolving the product in 1 M of NaOH solution at 60 °C overnight. The α-Fe_2O_3 nanospindles were synthesized by aging 20 mM $FeCl_3$ with 0.45 mM NaH_2PO_4 solution at 105 °C for 50 h.

Synthesis of multifunctional nanorattles

The samples are prepared *via* a modified method.[28] Four different solutions were prepared before the actual synthesis: 2 ml of tetraethyl orthosilicate (TEOS; reagent grade, 98%, Aldrich) with 18 ml of ethanol (solution A); 20 ml of ammonia solution (28%) and 60 ml of ethanol (solution B); 0.1 ml of N-[3-(Trimethoxysilyl)propyl]ethylenediamine (TSD; 97%, Aldrich) with 8 ml of ethanol (solution C); 0.1 ml of TEOS with 8 ml ethanol (solution D). 0.1 g of the as-prepared template, *i.e.*, SnO_2@SnO_2 hollow spheres or α-Fe_2O_3 nanospindles, were first dispersed in solution B. Then, 5 ml of solution A was slowly added into solution B under stirring. After 10 min, solution C and D were simultaneously added into the above reaction medium drop-by-drop over ~8 min, followed by the slow addition of the remaining solution A. After another 10 min, the product was washed and collected *via* centrifugation, and dried at 60 °C overnight. For the removal of the intermediate organosilica layer, 0.2 g of the as-prepared powder was dispersed in 20 ml of H_2O, followed by the addition of 0.75 ml of 10% hydrofluoric acid. The product was collected and washed after stirring for 10 min. For the functionalization of Au nanoparticles, 0.05 g of the complex nanorattles was dispersed in 3.5 ml of 0.04 M $HAuCl_4$, which was aged at 80 °C for 2 h. For the reduction of SnO_2 to Sn and α-Fe_2O_3 to Fe_3O_4, the samples were heated at 450 °C for 6 h and 400 °C for 9 h, respectively, under a dynamic flow of 5% H_2/95% N_2.

Materials characterization

The structure and morphology of the products were examined with Transmission Electron Microscopy (TEM; JEOL, JEM-2010, 200 kV). The elemental compositions of the samples were analyzed with energy-dispersive X-ray spectroscopy (EDX) attached to the field-emission scanning electron microscopy (FESEM; JEOL, JSM6340F). Crystallographic information of the samples was investigated with X-ray powder diffraction (XRD; Bruker, D8 - Advance X-Ray Diffractometer, Cu Kα, λ = 1.5406 Å). The surface area of the sample was measured using Quantachrome Instruments, Autosorb AS-6B, and the BET surface area was estimated using the adsorption data with the relative pressure ranging from 0.05 to 0.3.

Cell culture

MCF-7 cells were grown in Dulbecco's Modified Eagle's Medium (DMEM) (PAA Laboratories, Pasching, Austria) supplemented with 10% heat inactivated fetal bovine serum (PAA laboratories), 1 mM L-glutamine (Gibco, Grand Island, NY) and 50 U mL^{-1} penicillin/streptomycin (Gibco) in a humidified incubator with 5.0% CO_2 at 37 °C.

Cell uptake

Cells were seeded at a density of 1×10^5 cells cm^{-2} onto poly-L-lysine (0.1 mg mL^{-1}) coated coverslips for cell attachment overnight. To observe the cell uptake of nanoparticles, the cells were incubated with fluorescein isothiocyanate (FITC)-labeled Fe_3O_4@SiO_2@SiO_2. After 24 h, the cells were washed three times with a buffer and the fluorescence images were acquired by confocal laser scanning microscopy (CLSM) (LSM 510 META, Carl Zeiss, Germany).

Loading of DOX

2 mg of Fe_3O_4@SiO_2@SiO_2 was dispersed in 2 mL of aqueous doxorubicin (DOX) solution (0.05 mg mL^{-1}). After stirring for 24 h, the DOX-loaded sample was magnetically collected and

washed. The supernatants were collected for UV absorption measurement in order to determine the amount of DOX loaded.

Cell viability assay

The viability of the cells in the presence of nanoparticles was evaluated using the 3-[4,5-dimethylthialzol-2-yl]-2,5-diphenyltetrazolium bromide (MTT) assay. The MTT assay was performed in triplicate in the following manner. MCF-7 cells were seeded into 96-well plates at a density of 1×10^4 per well in 200 μL of media and grown overnight. The cells were then incubated at various concentrations of DOX, blank $Fe_3O_4@SiO_2@SiO_2$ or DOX-loaded sample for 24 h. Following this incubation, cells were incubated in media containing 0.5 mg mL^{-1} of MTT for 4 h. Thereafter, the MTT solution was removed and the precipitated violet crystals were dissolved in 200 μL of DMSO. The absorbance was measured at 570 nm using a BioTek microplate reader.

3. Results and discussion

Fig. 2A shows the transmission electron microscopy (TEM) image of the $SnO_2@SiO_2$ double-shell hollow spheres, which are quite uniform with a diameter of ~500 nm. The internal structure is clearly revealed with a coaxial orientation of the inner dark SnO_2 ring and the thicker SiO_2 outer shell. The intermediate organosilica layer can be facilely removed by treating the $SnO_2@SiO_2$ sample with dilute hydrofluoric (HF) acid (Fig. 2B).[28] During the dissolution process, mesopores will be created in the outer SiO_2 shell, and the resulting sample shows good structural robustness as no collapse is observed. At the same time, the structure evolves to a complex ball-in-ball structure, where a $SnO_2@SiO_2$ double-shell hollow sphere ~300 nm in diameter is confined inside a much larger SiO_2 hollow sphere with a distinct interstitial space in between. Au nanoparticles are then introduced into the empty region of the sample,[29] after which the inner SnO_2 is reduced to Sn. As depicted in Fig. 2C, the sample shows a very interesting rattle-in-ball structure, where the Sn nanoparticles ~100 nm in diameter are formed inside the inner SiO_2 shell, while this $Sn@SiO_2$ rattle structure can also be viewed as a complex core inside the outer SiO_2 shell, giving rise to a hollow structure with a multi-level interior architecture.[30,31] Such nanomaterials can probably be used in biological applications with improved mechanical, optical, as well as other properties.[31] More importantly, it is clear from the magnified image (Fig. 2D) that the interstitial space is functionalized with several Au nanoparticles a few nanometers in size. This type of structure could be more effective as a multifunctional nanoreactor than the normal nanorattles. In such situations, different reactants can easily diffuse *via* the mesopores in the outer SiO_2 shell into the large interstitial space, where they will probably react with one another with the reaction catalyzed by the incorporated noble metals, such as Au. At the same time, the inner-most core providing another functionality, *e.g.*, magnetism, will not affect the reaction process as it is well protected by a dense SiO_2 shell, making it inaccessible from the external medium. This could be a significant advantage of this type of hollow structure with a multi-level interior.

The X-ray diffraction (XRD) analysis confirms the full reduction of SnO_2 to Sn (see Fig. S1A, ESI†), as all the diffraction peaks can be indexed to metallic tetragonal β-Sn (JCPDS no. 04-0673). Due to the very small size and low mass fraction of the Au nanoparticles, no peaks owing to Au can be discerned from the pattern. However, the energy-dispersive X-ray analysis (EDX; Fig. S1B, ESI†) indicates the presence of a small amount of Au in the sample.

The versatility of the system is demonstrated by changing the starting template to α-Fe_2O_3 nanospindles, and uniform

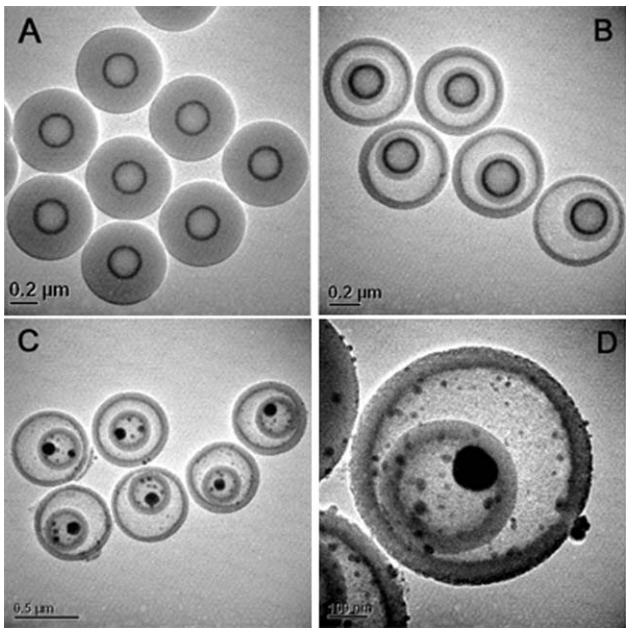

Fig. 2 Transmission electron microscopy (TEM) images of $SnO_2@SiO_2$ (A), $SnO_2@SiO_2@SiO_2$ after the removal of the organosilica layer in A (B), and $Sn@SiO_2@SiO_2$ with decoration of Au nanoparticles (C–D).

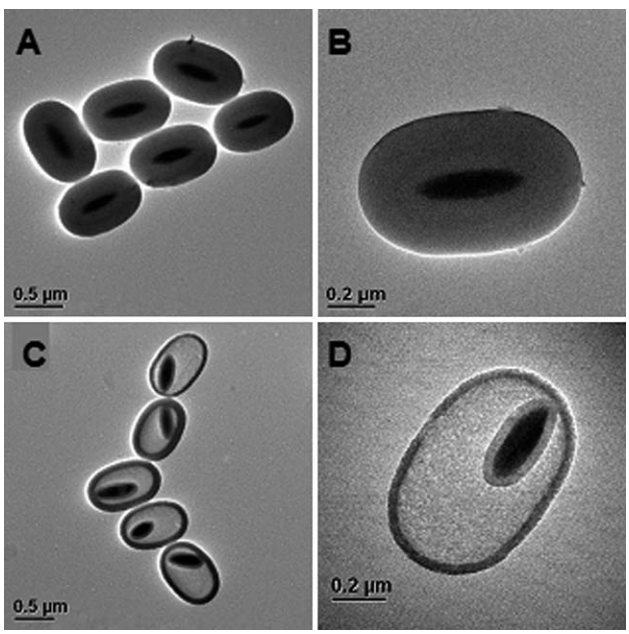

Fig. 3 TEM images of α-$Fe_2O_3@SiO_2$ (A–B), and α-$Fe_2O_3@SiO_2@SiO_2$ after the removal of the organosilica layer (C–D).

ellipsoidal α-Fe_2O_3@SiO_2 can be facilely obtained (Fig. 3A). These core-shell particles are ~800 nm in length and ~500 nm in width, and the α-Fe_2O_3 core can be easily identified inside the very thick SiO_2 shell (Fig. 3B). The intermediate organosilica layer can again be completely removed through HF treatment (Fig. 3C), giving rise to another type of complex rattle structure with a small α-Fe_2O_3@SiO_2 core and a thin SiO_2 outer shell of ~20 nm in thickness, and an unusually large interstitial space in between (Fig. 3D).

The XRD pattern (Fig. S2A, pattern I, ESI†) shows that the sample contains phase-pure rhombohedral Fe_2O_3 (JCPDS card no. 33-0664),[32] while the amorphous SiO_2 shell does not give any diffraction peaks. The magnetic functionality of the product is introduced by reducing the sample in H_2/N_2, and the α-Fe_2O_3 has been completely transformed into Fe_3O_4 after the treatment. This is confirmed by the XRD analysis (Fig. S2B, pattern II, ESI†), where all the identified peaks can be assigned to magnetite (JCPDS card no. 11-0614).[33] Such magnetic property of the sample allows it to be readily separated in an aqueous suspension (Fig S2A, inset, ESI†). The EDX analysis (Fig. S2B, ESI†) also confirms the presence of a small atomic fraction of Fe in the sample. The surface structure of the Fe_3O_4@SiO_2 rattles is subsequently studied, and the N_2 adsorption-desorption isotherm is given in Fig. S3, ESI.† It shows a distinct hysteresis loop, which signifies the possible presence of a mesoporous structure, and gives a surface area of 32 m^2 g^{-1}. From the pore size distribution, the mesopores are generally smaller than 10 nm.

Due to the high biocompatibility of SiO_2,[34] SiO_2-based nanomaterials have been widely studied in biological applications.[35–43] We have investigated the performance of these unique Fe_3O_4@SiO_2@SiO_2 nanorattles as a multifunctional carrier for drug delivery. Doxorubicin (DOX), a water-soluble anticancer drug, has been selected as a model drug against the MCF-7 cell line, a human breast carcinoma cell widely used in anticancer studies.[44,45] The cell uptake and biocompatibility of the Fe_3O_4@SiO_2@SiO_2 carriers were first verified by confocal laser scanning microscopy (CLSM). Fig. 4A–C shows the fluorescence, bright-field and merged images of MCF-7 cells incubated with fluorescein isothiocyanate (FITC)-Fe_3O_4@SiO_2@SiO_2 for 24 h, respectively. It is apparent from the images that the cells remained attached to the coverslip and also maintained their normal morphology after being incubated with the drug-free carrier, evidently proving that our Fe_3O_4@SiO_2@SiO_2 particles are highly biocompatible and non-cytotoxic. Moreover, strong green fluorescence can be observed inside the cytoplasm of the cells, which indicates a significant internalization of the nanoparticles,[40] suggesting the feasibility and efficiency of using Fe_3O_4@SiO_2@SiO_2 as a drug carrier. Furthermore, DOX can be loaded into the carrier with a high efficiency of 85%, which is demonstrated by the disappearance of the characteristic absorbance peaks in the UV-vis spectrum (Fig. S4, ESI†).

The anticancer efficacy of the DOX-loaded carrier is subsequently tested, with the result shown in Fig. 5. Consistent with the above CLSM analysis, the blank Fe_3O_4@SiO_2@SiO_2 causes insignificant damage to the MCF-7 cells when the sample concentration increases to 165 μg mL^{-1}, and the cell viability remains at 85% even at the highest concentration. More importantly, the DOX-loaded carriers exhibit a comparable or even better cytotoxicity compared to free DOX at each concentration level. Additionally, the Fe_3O_4 nanospindle core makes the sample suitable for T2 magnetic resonance imaging, which is commonly used to visualize the location of the drug carriers *in vivo*.[38] These results suggest that the as-prepared Fe_3O_4@SiO_2@SiO_2 nanorattles might serve as a highly efficient multifunctional drug delivery vehicle.

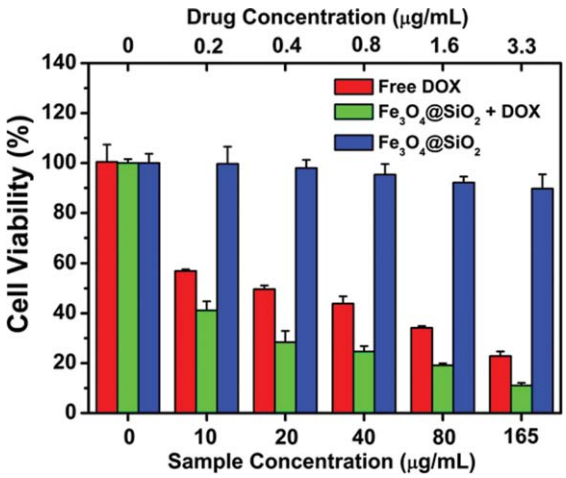

Fig. 5 *In vitro* cytotoxicity of free DOX, DOX-loaded Fe_3O_4@SiO_2@SiO_2, and blank Fe_3O_4@SiO_2@SiO_2 against MCF-7 cells after incubation for 24 h.

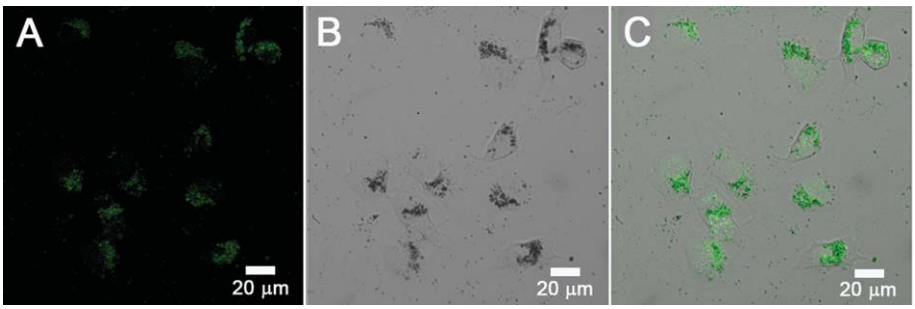

Fig. 4 Confocal laser scanning microscopic (CLSM) images of MCF-7 cells incubated with FITC-labeled Fe_3O_4@SiO_2@SiO_2 for 24 h. A: fluorescence; B: bright-field; C: the overlay image of A and B.

4. Conclusions

In summary, we have developed a new approach to generate complex rattle-type hollow nanostructures with multiple functionalities. Based on the platform of pure SiO_2 nanorattle, we are able to further engineer the core and the interstitial space, creating rattle-type structures with more complex architecture and chemical compositions compared to those reported previously. By starting with SnO_2 and Fe_2O_3 as two examples, we show that these unique multifunctional nanorattles can be used as efficient carriers for anticancer drugs, and probably advanced nanoreactors. Given the versatility of the current system, we believe that introduction of other functionalities into the rattle-type structures is possible, that will further expand the application potential of this unique nanostructure.

Acknowledgements

Y. Hu acknowledges the financial support from Zhejiang Provincial Natural Science Foundation of China (Y4110304) and Zhejiang Qianjiang Talent Project (2010R10025). X.W. Lou is grateful to the Nanyang Technological University and the Ministry of Education (Singapore) for financial support through the AcRF Tier-1 funding (RG 63/08, M52120096).

Notes and references

1 F. Caruso, R. A. Caruso and H. Möhwald, *Science*, 1998, **282**, 1111.
2 G. Decher, *Science*, 1997, **277**, 1232.
3 F. Caruso, R. A. Caruso and H. Mohwald, *Chem. Mater.*, 1999, **11**, 3309.
4 R. A. Caruso, A. Susha and F. Caruso, *Chem. Mater.*, 2001, **13**, 400.
5 Z. J. Liang, A. Susha and F. Caruso, *Chem. Mater.*, 2003, **15**, 3176.
6 K. Kamata, Y. Lu and Y. N. Xia, *J. Am. Chem. Soc.*, 2003, **125**, 2384.
7 P. M. Arnal, M. Comotti and F. Schuth, *Angew. Chem., Int. Ed.*, 2006, **45**, 8224.
8 G. Y. Liu, H. F. Ji, X. L. Yang and Y. M. Wang, *Langmuir*, 2008, **24**, 1019.
9 Y. Yin, Y. Lu, B. Gates and Y. Xia, *Chem. Mater.*, 2001, **13**, 1146.
10 X. W. Lou, C. L. Yuan, E. Rhoades, Q. Zhang and L. A. Archer, *Adv. Funct. Mater.*, 2006, **16**, 1679.
11 X. W. Lou, C. Yuan, Q. Zhang and L. A. Archer, *Angew. Chem., Int. Ed.*, 2006, **45**, 3825.
12 J. X. Zhu, T. Sun, H. H. Hng, J. Ma, F. Y. C. Boey, X. W. Lou, H. Zhang, C. Xue, H. Y. Chen and Q. Y. Yan, *Chem. Mater.*, 2009, **21**, 3848.
13 X. W. Lou, Y. Wang, C. L. Yuan, J. Y. Lee and L. A. Archer, *Adv. Mater.*, 2006, **18**, 2325.
14 T. Zhang, J. Ge, Y. Hu, Q. Zhang, S. Aloni and Y. Yin, *Angew. Chem., Int. Ed.*, 2008, **47**, 5806.
15 J. Li and H. C. Zeng, *J. Am. Chem. Soc.*, 2007, **129**, 15839.
16 J. S. Chen, C. M. Li, W. W. Zhou, Q. Y. Yan, L. A. Archer and X. W. Lou, *Nanoscale*, 2009, **1**, 280.
17 X. W. Lou, L. A. Archer and Z. C. Yang, *Adv. Mater.*, 2008, **20**, 3987.
18 Y. Q. Wang, G. Z. Wang, H. Q. Wang, W. P. Cai and L. D. Zhang, *Chem. Commun.*, 2008, 6555.
19 Z. Yang, Z. Niu, Y. Lu, Z. Hu and C. C. Han, *Angew. Chem., Int. Ed.*, 2003, **42**, 1943.
20 L. Zhang, S. Z. Qiao, Y. G. Jin, Z. G. Chen, H. C. Gu and G. Q. Lu, *Adv. Mater.*, 2008, **20**, 805.
21 X. W. Lou, C. L. Yuan and L. A. Archer, *Adv. Mater.*, 2007, **19**, 3328.
22 X. W. Lou, C. L. Yuan and L. A. Archer, *Small*, 2007, **3**, 261.
23 X. W. Lou and L. A. Archer, *Adv. Mater.*, 2008, **20**, 1853.
24 P. Jiang, J. F. Bertone and V. L. Colvin, *Science*, 2001, **291**, 453.
25 Y. Lu, Y. D. Yin and Y. N. Xia, *Adv. Mater.*, 2001, **13**, 271.
26 M. Kim, K. Sohn, H. Bin Na and T. Hyeon, *Nano Lett.*, 2002, **2**, 1383.
27 J. S. Chen, C. Chen, J. Liu, R. Xu, S. Z. Qiao and X. W. Lou, *Chem. Commun.*, 2011, **47**, 2631.
28 D. Chen, L. L. Li, F. Q. Tang and S. O. Qi, *Adv. Mater.*, 2009, **21**, 3804.
29 L. Tan, D. Chen, H. Liu and F. Tang, *Adv. Mater.*, 2010, **22**, 4885.
30 Z. Y. Wang, D. Y. Luan, C. M. Li, F. B. Su, S. Madhavi, F. Y. C. Boey and X. W. Lou, *J. Am. Chem. Soc.*, 2010, **132**, 16271.
31 Y. Zhao and L. Jiang, *Adv. Mater.*, 2009, **21**, 3621.
32 J. S. Chen, T. Zhu, C. M. Li and X. W. Lou, *Angew. Chem., Int. Ed.*, 2011, **50**, 650.
33 C. J. Jia, L. D. Sun, F. Luo, X. D. Han, L. J. Heyderman, Z. G. Yan, C. H. Yan, K. Zheng, Z. Zhang, M. Takano, N. Hayashi, M. Eltschka, M. Klaui, U. Rudiger, T. Kasama, L. Cervera-Gontard, R. E. Dunin-Borkowski, G. Tzvetkov and J. Raabe, *J. Am. Chem. Soc.*, 2008, **130**, 16968.
34 C. Barbe, J. Bartlett, L. G. Kong, K. Finnie, H. Q. Lin, M. Larkin, S. Calleja, A. Bush and G. Calleja, *Adv. Mater.*, 2004, **16**, 1959.
35 L. Li, F. Tang, H. Liu, T. Liu, N. Hao, D. Chen, X. Teng and J. He, *ACS Nano*, 2010, **4**, 6874.
36 Y. Chen, H. Chen, D. Zeng, Y. Tian, F. Chen, J. Feng and J. Shi, *ACS Nano*, 2010, **4**, 6001.
37 J. Kim, J. E. Lee, J. Lee, J. H. Yu, B. C. Kim, K. An, Y. Hwang, C.-H. Shin, J.-G. Park, J. Kim and T. Hyeon, *J. Am. Chem. Soc.*, 2005, **128**, 688.
38 J. E. Lee, N. Lee, H. Kim, J. Kim, S. H. Choi, J. H. Kim, T. Kim, I. C. Song, S. P. Park, W. K. Moon and T. Hyeon, *J. Am. Chem. Soc.*, 2009, **132**, 552.
39 Y. Deng, Y. Cai, Z. Sun, J. Liu, C. Liu, J. Wei, W. Li, C. Liu, Y. Wang and D. Zhao, *J. Am. Chem. Soc.*, 2010, **132**, 8466.
40 T. Wang, F. Chai, Q. Fu, L. Zhang, H. Liu, L. Li, Y. Liao, Z. Su, C. Wang, B. Duan and D. Ren, *J. Mater. Chem.*, 2011, **21**, 5299.
41 Y. Chen, H. Chen, M. Ma, F. Chen, L. Guo, L. Zhang and J. Shi, *J. Mater. Chem.*, 2011, **21**, 5290.
42 J. Liu, S. Z. Qiao, S. Budi Hartono and G. Q. Lu, *Angew. Chem., Int. Ed.*, 2010, **49**, 4981.
43 Y. Chen, H. Chen, L. Guo, Q. He, F. Chen, J. Zhou, J. Feng and J. Shi, *ACS Nano*, 2010, **4**, 529.
44 X. T. Zheng and C. M. Li, *Biosens. Bioelectron.*, 2010, **25**, 1548.
45 X. T. Zheng, H. B. Yang and C. M. Li, *Anal. Chem.*, 2010, **82**, 5082.

